

AERODYNAMIC DESIGN AND STUDY OF WIND TURBINE BLADE AEROFOIL

Pradeep Vishwakarma¹, Arun Singh Patel²

¹P.G scholar, Mechanical Engineering, NRI Institute of Information Science and Technology, Bhopal

²H.O.D, Mechanical Engineering, NRI Institute of Information Science and Technology, Bhopal

Abstract: The general aim of this project was to get a better understanding of the physical behaviour of the flow field past wind turbine rotors, including the boundary layer flow as well as the wake region. Although CFD is not a practical design tool, useful suggestions for classical design methods can be derived from the analysis. A design method with reference to modeling in Uni-graphics and proceeded by simulation by using CFD (Computational Fluid Dynamics) Star CCM+ program is chosen for current work, so that the expense and time needed to find optimum aerodynamic design of a wind turbine blade by experiment can be minimized. NREL-S809 CFD models are presented using Star CCM+ software. Using the Spalart-Allmaras turbulent viscosity, the dimensionless lift, drag and pitching moment coefficients were calculated for wind-turbine blade at different angles of attack. These CFD model values we then validated using published calibrated lift and drag coefficients evident in the literature. Optimum values of these coefficients as well as a critical angle were found from polar curves of lift, drag and moment modelling data. These data were exploited in order to select the aerofoil with best aerodynamic performance for basis of a three-dimensional model analogue. Thereafter a three-dimensional CFD model of small horizontal axis wind-turbine was produced.

Key words: Wind energy, wind turbine aerodynamics, CFD-RANS, blade design, wakes.

Introduction

In general, the lift on an airfoil is primarily the result of its angle of attack and shape. When oriented at a suitable angle, the airfoil deflects the oncoming air, resulting in a force on the airfoil in the direction opposite to the deflection. This force is known as aerodynamic force and can be resolved into two components: Lift and drag is the force used to overcome gravity and is defined to be perpendicular to direction of the oncoming airflow.[1] It is formed as a consequence of the unequal pressure on the upper and lower airfoil surfaces. The drag force is defined as a force parallel to the direction of oncoming airflow. The drag force is due to both viscous friction forces at the surface of the aero

foil and unequal pressure on the airfoil surfaces facing toward and away from the oncoming flow.[2] The lift is the force used to overcome gravity and the higher the lift the higher the mass that can be lifted off the ground. For an aero foil the lift to drag ratio should be maximum. As a result, it can improve efficiency when wind turbine generates electricity. Lift and drag coefficients C_L and C_D are defined as follows.

LIFT COEFFICIENT-

$$C_L = \frac{Fl}{\frac{1}{2}\rho V^2 C}$$

DRAG COEFFICIENT-

$$C_D = \frac{Fd}{\frac{1}{2}\rho V^2 C}$$

Where,

ρ = Density of the air

c = The length of the aero foil, often denoted by the chord

V = The velocity of air

F_L = Forces acting on aero foil unit for the lift in equations (N/m).

F_D = Forces acting on aero foil unit for the drag in equations (N/m).

Indian Wind Energy Status

Wind power program began in India at the end of five-sixths of the annual plans for 1983-1984 and in recent years has increased dramatically. The main objective of the program was to commercialize the production of wind energy, support for research and development, provide assistance to wind projects and awareness. Under this program, the Ministry of Non-Renewable Energy (MNRE) has made several changes regarding incentives, plans and policies for wind power. Twenty years have passed since the shape of the world's first offshore wind power Vinde by (5 MW), was built in Denmark. Today, 4,620 MW of offshore wind power was installed worldwide, accounting for approximately 2% of the total installed capacity of wind power. Over 90% of it is installed outside Northern Europe, in the North, Baltic and Irish Seas and the English Channel. Most of the rest is in two demonstration projects on the east coast of China. However, there are also high for greater deployment expectations elsewhere, governments and businesses in Japan, Korea, USA, Canada, Taiwan and even India have shown enthusiasm for offshore development in its waters. India is a newcomer to the

wind industry compared with Denmark or the USA. But the policy support of the Indian wind energy has led India and ranks fifth capacity most installed wind power. The total installed capacity of 19,565 MW was 30 June 2013 [3]. And now India is just behind the United States, China, Spain and Germany. The total installed capacity of wind power shows a better performance of India in the field of wind energy (Table 1.1). The top five countries of wind energy are China, USA, Germany, Spain and India, which together represent 73 percent of the global wind capacity. The total installed wind power capacity in India reached 17.9 GW in August 2012 the total capacity added in 2012 was around 1700 total installed capacity MW 2013 in India and 2011 is illustrated rapid growth of installation of wind power was measured in the southern and western India. One needs about 350-360 GW of total capacity of power generation has been reported by the Central Electricity Authority in its national plan for electricity (2012), for the year 2022 [4]. Wind potential onshore only has hitherto been used by India. Despite the fact that India has a coastline 7,500 km, we have not yet taken advantage of our offshore wind resources for electricity generation.



Fig. 1 NTK500/41 [1]

Due to the development of computer aided design codes, they provide another way to design and analyses the wind turbine blades. Aerodynamic performance of wind turbine blades can be analyzed using computational fluid dynamics (CFD), which is one of the branches of fluid mechanics that uses numerical methods and algorithms to solve and analyze problems of fluid flows. [5] Meanwhile, finite element method (FEM) can be used for the blade structure analysis. Comparing to traditional theoretical and experimental methods, numerical method saves money and time for the performance analysis and optimal design of wind turbine blades.

An aero foil is the shape of a wing or blade (of propeller, rotor, or turbine) or sail as seen in cross-section.

An airfoil-shaped body moved through a fluid produces an aerodynamic force. The component of this force perpendicular to the direction of motion is called lift. The component parallel to the direction of

motion is called drag. Subsonic flight airfoils have a characteristic shape with a rounded leading edge, followed by a sharp trailing edge, often with asymmetric camber. [6]

Foils of similar function designed with water as the working fluid are called hydrofoils. Before introducing the aero foil behavior, Mach number and Reynolds number need to be explained. [7] Mach number is a ratio of speed of an object over sound and it is defined as:

$$M = \frac{v}{v_{\text{sound}}}$$

Where,

v = velocity of object

v_{sound} = velocity of the sound in the medium

The Reynolds number is a non-dimensional value and it is a ratio of inertial force to viscous force, defined as:

$$Re = \frac{\text{inertial forces}}{\text{viscous forces}} = \frac{\rho v L}{\mu} = \frac{v L}{\nu}$$

Where,

V is the mean velocity of the object relative to the fluid.

L is a characteristic linear dimension.

μ is the dynamic viscosity of the fluid.

ρ is the [density](#) of the fluid

AERO FOIL BEHAVIOR

It is indispensable to study the aero foil behavior: aerodynamic performances are different because of different geometry of aero foil, and choosing an applicable aero foil for wind turbine blade will improve the efficiency. Here we are using NREL S807 and S809 aero foil.

Recent development of the computational fluid dynamics (CFD) allows us to simulate overall flow around HAWT (horizontal axis wind turbine) using RANS (Reynolds average Navier–Stokes) model and overset grids to facilitate the simulation of flows about complex configurations. Though the state of the art CFD is needed considerable computer power and validations for Navier–Stokes model. CFD based on turbulent flows are characterized by fluctuating velocity fields. [9] These fluctuations mix transported quantities such as momentum, energy and species concentration, and cause the transported quantities to fluctuate as well.

CFD Analysis

Comprehensive overviews of the techniques used to solve problems in fluid mechanics on Computers is given in. In commercial codes a friendly interface gives the user the possibility of easy setting the various options and analyzes the results. Three large parts are generally indicated of a CFD code, which correspond to three phases of the problem analysis:

PREPROCESSOR: In this phase the physical problem is implemented into the mathematical model. The Computational domain is now defined. Then, it is divided into a certain number of elements, which constitute the mesh or grid. The fluid properties and the



boundary conditions are set. Since the CFD solution of a fluid dynamic problem is given locally, for well-defined positions within computational grid, the global accuracy strongly depends on the total number of mesh elements. A rule-of-thumb says that the larger is the number of elements; the better is the solution accuracy, even though CPU effort and the total time of convergence will be higher as well. Consequently, the optimal grid should be finer where higher are the variables gradients and coarser in the region characterized by smooth changes in the flow. The final success of a CFD simulation strongly depends on the preprocessing and therefore a special attention needed to paid to the choice of the mesh and of boundary conditions. [10,11]

The remainder of the paper was organized as follows: Section 2 explains the modelling and meshing of the NREL Phase VI rotor using STAR CCM+, boundary conditions and computational time. Section 3 explains the details of NREL Phase VI rotor. Section 4 describes the results from CFD and comparison with experimental data and finally Section 5 gives the summary of the findings and relevant conclusions of the present work.[11]

2. Methodology

The numerical solution algorithm is the core of a CFD code. All the main CFD solvers work with the following procedure:

1. Modeling the problem unknowns by means of simple analytical functions and discretizing the governing equations for the fluid flows, properly modified by substituting the mentioned functions.

2. Solving the algebraic system of equations.

Most of the commercial CFD codes are based on a finite volume discretization and perform these operations:

- Integrating the governing equations over each control volume within the computational domain. We obtain the resulting equations in terms of flux.

- Discretizing: the flux terms, which deal with convection and diffusion processes, are approximated with a finite differential approach as well as the source terms in order to obtain an algebraic system of equations. [12]

- Solving the algebraic system of equations with iterative methods.

POSTPROCESSING: Under this definition we include the analysis of solution results. The solver output is a set of solution variables, associated to the given grid nodes or volumes. These data must be collected, elaborated in the most suitable way for the analysis, in order to produce a physical representation of the solution. Star CCM+ software having a post-processing section.[13] It able to do the following post-processing operations:

- Domain and grid visualization
- Vectorial plots of solution variables
- Linear, surface, volume integrals
- Iso-level and contour plots of solution variables, within selected domain zones
- Drawing two-dimensional and three-dimensional plots

- Tracking path-lines, stream traces, etc.

- Algebraic and analytical operations within the variables

- Dynamic representations, animations etc.

Two Dimension Model Simulations

The two dimension simulation proposed to obtain airfoil characteristics which will be used in blade design with angle of attack variation. Two dimension simulation processes is completed by meshing and iteration using star ccm+ with assumption of compressible flow and segregated solver was used including energy calculation using absolute velocity formulation in steady condition.[14] These assumptions are requisite in order to obtain accurate current model on airfoil surface by showing turbulence phenomenon, flow separation, boundary layer, and reversed flow. This flow phenomenon is their natural flow characteristic, where the decrease in whole airfoil performance and rotor efficiency in extreme situation. For both airfoils taking chord length as 1 m. and far field dimensions taken as 20 times in back of aero foil 10 times in front of aero foil. Total 30 times in terms of length, and 20 times in terms of width from an aerofoil. So aero foil far field will be 30m in length and 20 m in width. [15]

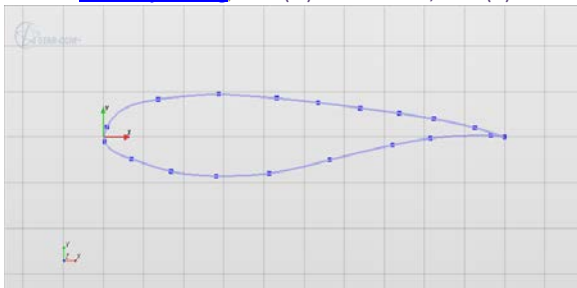
After making the far field domain we converted this region to 2d region with same meshes and dimensions, for simplicity 2d region also give the same result for these two aero foils. Now these two aero foils analyses with angle of attacks of 0 deg, 2deg, 4deg, 6 deg, 8deg, 10deg, 11deg, 12deg, 13deg, 14deg, 15deg, 16deg.

Problem Statement

The project was aimed at finding the lift and drag coefficient for two NREL aero foils S807 and S809. comparing them to find which is more suitable for making wind turbine blades. Wind turbines operate in the lowest part of the atmospheric boundary layer, where steady wind is an off-design condition, so that wind turbine aerodynamics is essentially unsteady. Unlike most of the aerodynamic devices, wind turbine does not avoid stall, but rely on it for limiting power (e.g. in the classical Danish-concept turbines): a thorough understanding of unsteady deep stall is hence necessary. [16]

MODELING: Moreover, the flow past a wind turbine blade is three-dimensional, particularly in the blade-tip and root region. For instance centrifugal and Coriolis forces are experienced by the boundary layer flow, mainly in the inboard, causing a stall-delay effects, by which higher lift is achieved compared to two-dimensional data.[17]

For NREL S807



For NREL S809

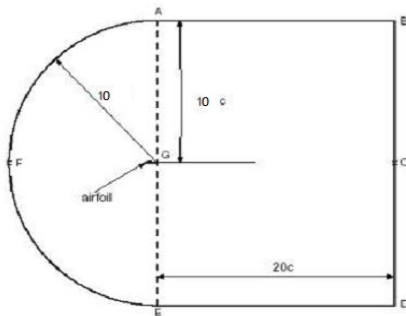
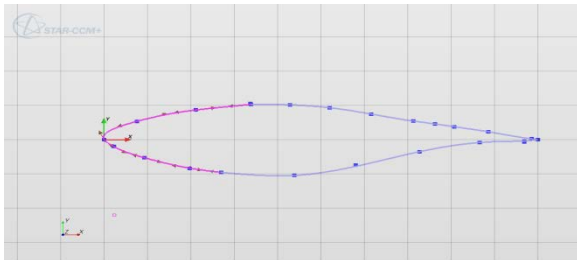


Figure 1 Aero foil position in far field

SETTING UP THE MESH

STAR CCM+ is having different kind of like meshes and region based meshing is used. We are using following type of meshes. First we have to select the base size for the model. The Base Size is a characteristic dimension of the model that you set before using any relative values here base size is taken as 1m.using any relative values. [18] Two different kind of mesh is used to generate mesh for this project.

SURFACE REMESHER

In order to improve the overall quality of an existing surface and optimize it for the volume mesh models, the surface re-mesher can be used to re-triangulate the surface. The re-meshing is primarily based on a target edge length that you supply and can also include feature refinement that is based on curvature and surface proximity. Localized refinement that is based on part surfaces or boundaries can also be included. Specific surfaces or boundaries can also be omitted from the process so that the original triangulation from the imported mesh can be preserved. [19] The surface re-mesher is typically used for re-meshing surfaces that are output from the surface wrapper and STL type data. As well as improving the surface for the volume meshers it also aids the subsurface generator when the prism mesher option is selected.

Volumetric control included as part of the surface re-meshing operation. This option allows the surface target size to be set for any of the allowable shapes that encompass the import surface. Here target size is given 0.15m, and minimum size is 0.10m.

PRISM LAYER MESH

The prism layer mesh model is used with a core volume mesh to generate orthogonal prismatic cells next to wall surfaces or boundaries. This layer of cells is necessary to improve the accuracy of the flow solution. A prism layer is defined in terms of:

1. Its thickness
2. The number of cell layers within it.
3. The size distribution of the layers.

The function that is used to generate the distribution either by geometric progression or hyperbolic tangent. These general properties can be defined globally within an automated mesh operation or a mesh continuum, and can also be defined locally on part surfaces, regions, or boundaries, and within volumetric controls. Here thickness of prism layer is taken as 0.003m, and number of prism layers taken as 20 to catch the boundary interaction.

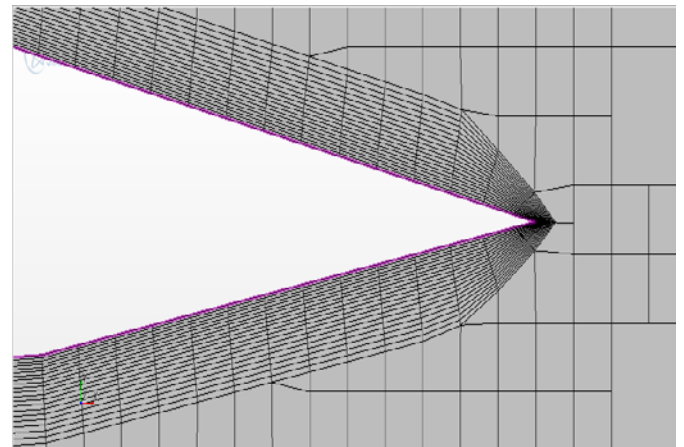


Figure 2 Prism layer mesh

VOLUMETRIC CONTROL FOR MESH

A volumetric control to specify the mesh density in a specific zone for both surface and volume meshes. You can define the mesh refinement zone using volume shapes and geometry parts. You can apply each volumetric control to any combination of meshing models. Therefore, you can set specific cell sizes within the zone for each mesh generation stage. Volumetric controls can overlap and extend outside the region boundary definition. Volumetric controls can also overlap from one region to another, but the effect is only included if the region belongs to the same mesh continuum as the volumetric control. If two or more volumetric controls overlap, the smallest user-defined cell size takes priority. The relevant growth rate for each core mesh model determines the transition in cell sizes from the volumetric control to the core mesh.

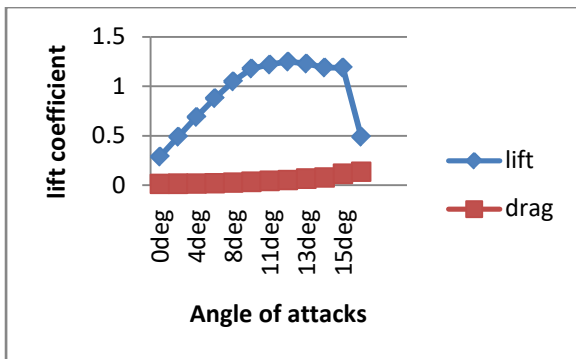
Different type of volumetric control shapes are used according to our requirement like block cone, cylinder. Here block shape is used to catch the geometry.

This block is used to capture shape of the geometry of aerofoil. So fine mesh is used with the size of 0.005m.for

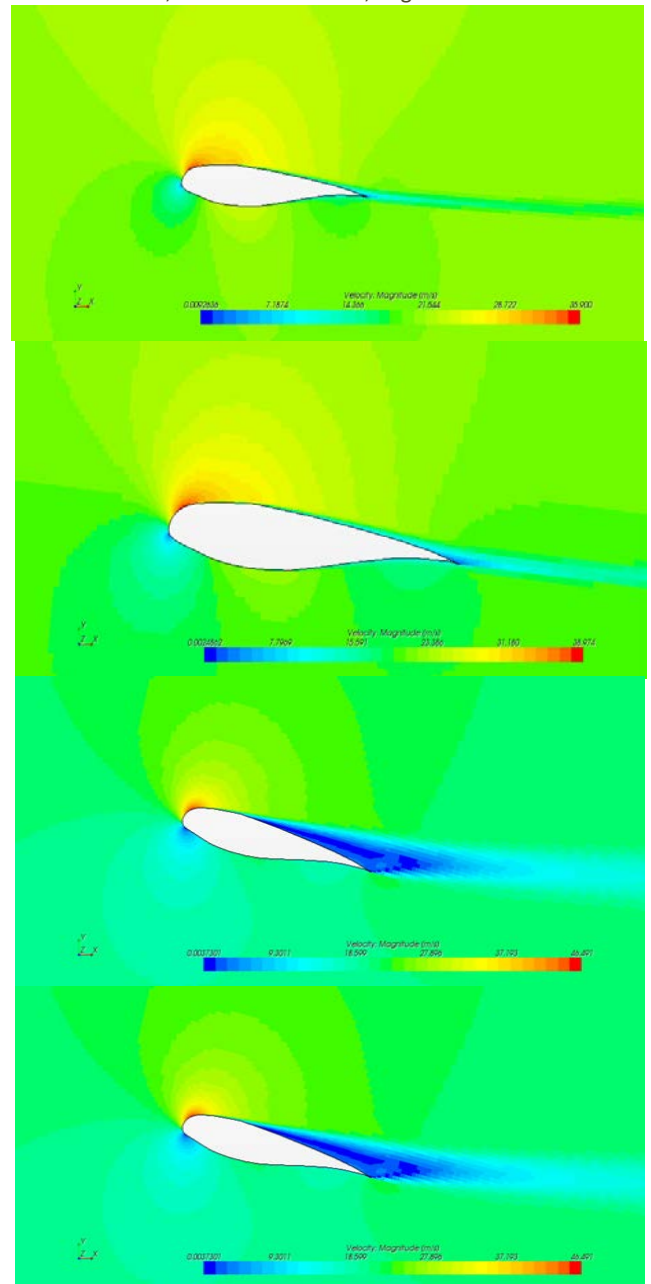
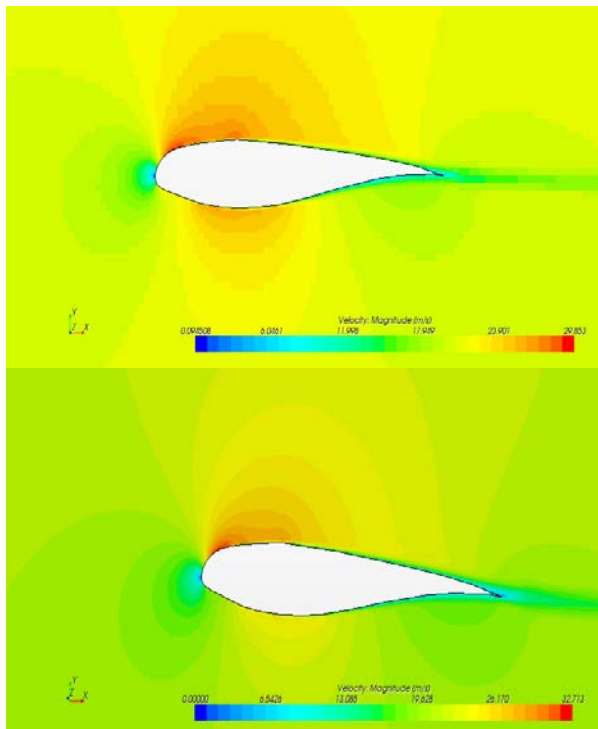
surface and volume mesh. This is necessary because its shape and to wall where the flow detachment happens.

4. Results and Discussion

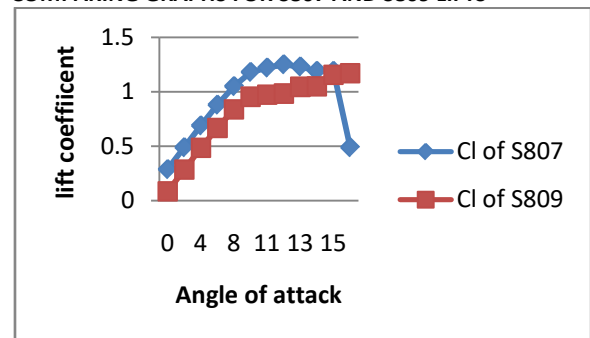
The graph below shows lift is increasing as increasing the angle of attack but this will also increase drag. For getting accurate angle after 10 deg , 1deg changes results have calculated this will give maximum lift angle as graph shows maximum lift is around 16 deg but at that point drag is also increase and flow become more detached. So instead of that taking 15 deg as maximum lift 1.049 because its not having much detached flow and drag is also less at 0.0848 compare to 16degs.0.176.



Graph for aero foil S809 C_l vs C_d
FOR AEROFOIL S809 –



COMPARING GRAPHS FOR S807 AND S809 LIFTS



Conclusion

The aim of the project was to produce a review and to get a better understanding of wind turbine blades aerodynamics, by means of a wide-range CFD-RANS



simulation campaign. Several issues were addressed. The boundary layer and the near wake flow. The results from the computations were quite satisfactory and, in our opinion, they can represent a good foundation for future work in this area. The more significant findings are summarized below.

1. Using the second order SST $k-\omega$ turbulent model, Star CCM+ shows a good agreement with the measured data for a wind speed 20m/s. For NREL S807 maximum lift is 1.25 at angles of attack 12deg. further increasing AOA gives drop in lift and drag is increasing to 0.134.
2. For NREL S809 maximum lift of 1.155 at 16 deg. With high drag of 0.176.
3. It also concludes that aero foil S807 is useful in near hub of wind turbine blade and aero foil S809 which have greater range of flow acceptability can be used for main blade area up to tip of blade.

Reference:

[1] NTK500/41
http://130.226.17.201/extra/web_docs/nordtank/WT_description.pdf

[2] Hasen M., 2000, "Aerodynamics of Wind Turbines"

[3] Larsen, J., "STAR CCM+ CFD Applied to Wind Turbines at Siemens Wind Power," STAR CCM+ Conference & 26th CADFEM Users' Meeting, Darmstadt, Germany, October 2008.

[4] Mark A. Potsdam, Dimitri J. Mavriplis, "Unstructured Mesh CFD Aerodynamic Analysis of the NREL Phase VI Rotor", AIAA 2009-1221, 47th AIAA Aerospace Sciences Meeting Including The New Horizons Forum and Aerospace Exposition, 5 - 8 January 2009, Orlando, Florida.

[5] Le Pape, A., and Gleize, V., "Improved Navier-Stokes Computations of a Stall-Regulated Wind Turbine Using Low Mach Number Preconditioning," 44th AIAA Aerospace Sciences Meeting and Exhibit, Reno, NV, January 2006, AIAA 2006-1502.

[6] Robin Langtry, Florian Menter, "Overview of Industrial Transition Modelling in CFX", STAR CCM+ Germany GmbH, STAR CCM+ CFX.

[7] Standish, K. J., and van Dam, C. P., "Aerodynamic Analysis of Blunt Trailing Edge Airfoils," Journal of Solar Energy Engineering, Vol. 125, No. 4, Nov. 2003, pp. 479-487.

[8] Fuglsang, P., and Bak, C., "Development of the Risø Wind Turbine Airfoils," Wind Energy, Vol. 7, No. 2, May 2004, p. 145-162.

[9] M.M. Hand, D.A. Simms, L.J. Fingersh, D.W. Jager, J.R. Cotrell, S. Schreck, and S.M. Larwood, "Unsteady Aerodynamics Experiment Phase VI: Wind Tunnel Test Configurations and Available Data Campaigns", NREL/TP-500-29955, December 2001.

[10] Johansen, J., Sørensen, N. N., Michelsen, J. A., and Schreck, S., "Detached-Eddy Simulation of Flow around the NREL Phase-VI Rotor," Wind Energy, Vol. 5, No. 2-3, 2002, pp. 185-197.

[11] Johansen J., Madsen, H. A., Sørensen, N. N., and Bak C., "Numerical Investigation of a Wind Turbine Rotor with an Aerodynamically Redesigned Hub-Region," 2006

European Wind Energy Conference and Exhibition, Athens, Greece, 2006.

[12] Johansen J., and Sørensen N. N.: "Aerodynamic investigation of winglets on wind turbine blades using CFD", Risø-R- 1543(EN) report 2006.

[13] Hansen, M. O. L., and Johansen, J., "Tip Studies Using CFD and Comparison with Tip Loss Models," Wind Energy, 2004, p. 343 -356.

[14] Hjort, S., Laursen, J., and Enevoldsen, P., "Aerodynamic Winglet Optimization," Sandia National Lab Blade Workshop, May 2008.

[15] Duque, E. P. N., Burklund, M. D., and Johnson, W., "Navier-Stokes and comprehensive analysis performance predictions of the NREL phase VI experiment," Journal of Solar Energy Engineering 2003; 125: 457-467.

[16] Chao, D. D., Van Dam, C. P., "Computational Aerodynamic Analysis of a Blunt Trailing-edge Airfoil Modification to the NREL Phase VI Rotor," Wind Energy, July 2007, 10:529-550.

[17] Menter FR. "Two-equation eddy-viscosity model for engineering applications". AIAA-Journal 1994; 32(8):1598-1605.

[18] Gonzalez A., Munduate, X., "Three-dimensional and Rotational Aerodynamics on the NREL Phase VI Wind Turbine Blade," 45th AIAA Aerospace Sciences Meeting and Exhibit, Reno, NV, January 2007, AIAA 2007-0628.

[19] Schmitz, S., Chattot, J-J., "Application of a 'Parallelized Coupled Navier-Stokes/Vortex Panel Solver' to the NREL Phase VI Rotor," 43rd AIAA Aerospace Sciences Meeting and Exhibit, Reno, NV, January 2003, AIAA 2003-0593.